

PERIODICO di MINERALOGIA
established in 1930

*An International Journal of
MINERALOGY, CRYSTALLOGRAPHY, GEOCHEMISTRY,
ORE DEPOSITS, PETROLOGY, VOLCANOLOGY
and applied topics on Environment, Archaeometry and Cultural Heritage*

Technological analysis of Sicilian prehistoric pottery production through small angle neutron scattering technique

Simona Raneri^{1*}, Germana Barone¹, Vincenza Crupi², Francesca Longo², Domenico Majolino², Paolo Mazzoleni¹, Davide Tanasi³, José Teixeira⁴ and Venuti Valentina²

¹ Dipartimento di Scienze Biologiche, Geologiche e Ambientali, Università di Catania, Corso Italia 57, 95125 Catania, Italy

² Dipartimento di Fisica e di Scienze della Terra, Università di Messina, Viale F. Stagno D'Alcontres 31, 98166 Messina, Italy

³ Arcadia University, The College of Global Studies, Via Roma 124, 96100 Siracusa, Italy

⁴ Laboratoire Léon Brillouin (CNRS/CEA), CEA Saclay, 91191 Gif-sur-Yvette Cedex, France

*Corresponding author: sraneri@unict.it

Abstract

The Middle Bronze Age in Sicily (15th-13th century BC) represents a crucial moment in the evolution of Prehistoric pottery production. However, the scarcity of specific petrographic and chemical studies has represented until now a serious interpretative handicap for archaeologists. The recent study of an important Middle Bronze Age pottery complex from the site of Grotte di Marineo (Licodia Eubea, Catania), offers the possibility to add new significant data in this field. The analyses, carried out on a group of diagnostic samples representing 13% of the whole complex, allowed us to obtain a precise characterization that surpassed the misleading identification based on the simple autoptical exam.

This paper highlights the potentiality of the small angle neutron scattering (SANS) technique as a non-invasive analytical tool for the study of technological aspects, in conjunction with other, more usual, methodologies such as scanning electron microscopy (SEM), in order to better investigate production technology of Middle Bronze Age Sicilian pottery.

Key words: Middle Bronze Age; pottery technology; pyrotechnology; SANS; SEM.

Research goals

The goal of this study is to highlight, for the first time, the evolution of technological aspects

of Sicilian Prehistoric pottery manufacture through three chronological sub-phases, in which the local Middle Bronze Age can be divided. A group of Middle Bronze Age

pottery was selected from the cave site of Grotte di Marineo (Licodia Eubea, Catania, Italy). Preliminary mineralogical analysis and petrographic classification on the same set of samples are reported in Barone et al., (2011a).

In this research, the knowledge about the micro-destructive and non-invasive analytical techniques developed during the PRIN2007 financial support have been applied.

In particular, the structural characterization of the samples was performed at different scales of observation. The macroscopic features of the pottery was carried out by detailed microscopic petrographic and scanning electron microscopy (SEM) investigations, while mesoscopic features were obtained by SANS measurements. In addition, geochemical composition was been obtained by X-ray fluorescence analysis (XRF). Finally, these original data integrate the X-ray diffraction (XRD) and Fourier transform infrared spectroscopy (FT-IR) results about the microscale features of samples, reported in a previous paper (Barone et al., 2011a). This analytical approach allowed to obtain detailed and complete information on the production technology of

the studied samples. The obtained results, in the frame of a wider research project, still ongoing on the technological analyses and archaeometric characterizations of Sicilian Middle Bronze Age pottery, have emphasized the importance of SANS as reliable non-invasive technique of analysis.

Introduction

An on going problem of the archaeological research on Sicilian Prehistoric pottery is represented by a general lack of data about the technological features of the production and the petrographic and geochemical characterization. In particular, the only studies available on the Middle Bronze Age are those about the Aeolian islands (Levi et al., 2005; Williams et al., 2000).

The Sicilian Middle Bronze age, corresponding with Thapsos culture, has a chronological development different from that of the Italian Peninsula, as clarified in Table 1. The pottery production of this period shows a certain degree of experimentalism bringing to a prominent technical evolution that firmly established

Table 1. Comparative chronological chart of Early and Middle Bronze Ages in Sicily, Southern Italy and the Aegean.

CHRONOLOGY	SICILY		SOUTHERN ITALY	AEGEAN
ca. 2200/2100 - 1440/1420 BC	Early Bronze Age	Castelluccio	Early Bronze Age 1-2 Middle Bronze Age 1-2	MH - LH II
1440/1420 - 1400/1380 BC		Thapsos I	Middle Bronze Age 3	LH IIIA1
1400/1380 -1310/1300 BC	Middle Bronze Age	Thapsos II	(<i>Apennine</i>)	LH IIIA2
1310/1300 -1270/1250 BC		Thapsos III	Late Bronze Age 1 (<i>Sub-Apennine</i>)	LH IIIB1

some standards in every phases of the operative chain, from clay selection to manufacture, from decoration to firing.

The arrival in Sicily of LH IIIA/IIIB Mycenaean and Cypriote fine ware can be identified as the turning event that affected the behavior of the local artisans, inspiring them to further achievements (La Rosa, 2004).

The repertoire and the features of the Thapsos pottery are mainly known thanks to the explorations of several cemeterial contexts of Siracusa territory carried out by Paolo Orsi between the end of the 19th and the first decade of the 20th century (Leighton, 1986).

Since the work of Orsi did not focus so much on the territory of Catania, with the exception represented by the excavation of the prehistoric site of Barriera (Orsi, 1907a; Procelli, 2007), it has been not possible to undertake any interpretative analysis about Thapsos pottery production in this area. Just in the past decade, thanks to new researches (Procelli, 1992; Privitera, 2010) and excavations both in the Catania (Branciforti, 1999; Tanasi, 2010) and

its province, as Valverde (Branciforti, 1999) and Caltagirone (Tanasi, 2008), new discoveries contributed to the definition of a peculiar production of Aetnean Thapsos pottery - label indicating the pottery manufactured in the areas surrounding the Aetna volcano nearby Catania - to be compared and contrasted to the Siracusan Thapsos pottery, the only traditional known.

The present paper is part of a more articulated research project on the typological, stylistic and technical analysis of the Thapsos pottery of Catania territory, where for the first time great emphasis is given to the archaeometric characterization of the ceramics (Barone et al., 2011b).

The specimens discussed in this contribute come from the site of Grotte di Marineo, located on the northern slope of Marineo Mount, in the municipality of Licodia Eubea (Catania), even if it is closer to the town of Grammichele (Figure 1). The site, explored by the Superintendence of Cultural Heritage of Catania between 1988 and 1989 (Consoli, 1988-1989), consists of four natural caves, three of

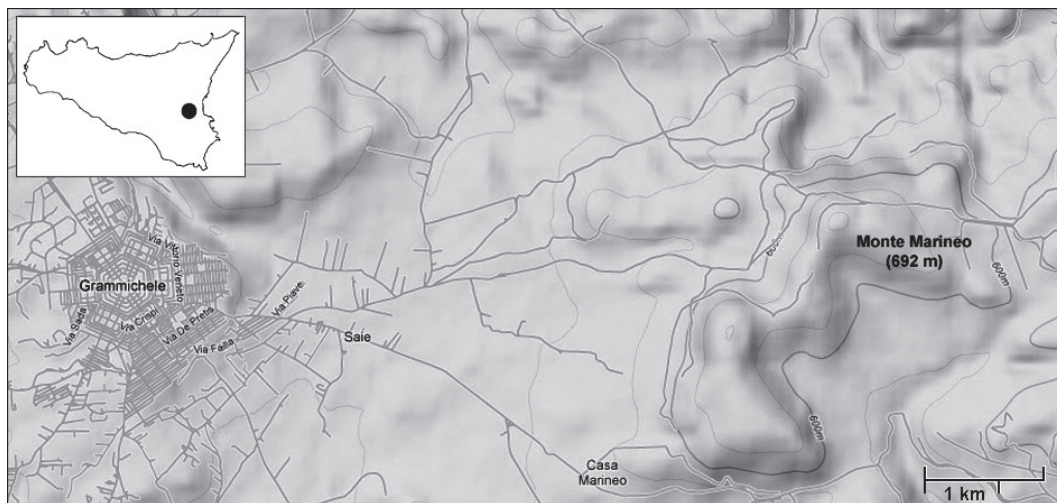


Figure 1. Plan of the suburban area of Grammichele and Monte Marineo (Sicily).

which are in State property (Cave 1, 2 and 4), while the fourth (Cave 3) is in private property (proprietà Cucuzza).

Caves 1 and 3 produced the most relevant data, although the excavations were not carried out following the stratigraphic criteria and without a proper graphic and photographic documentation. The pottery found testified to a continuous occupation from the Neolithic (*Diana facies*) to the 6th century BC, with a gap just in the Late Bronze Age (North Pantalica *facies*).

To infer an hypothesis about the use of the caves of Grotte di Marineo during the Middle Bronze Age could be rather risky both for the absence of a scientific method of excavation and for wide ranges of problems concerning the interpretation of cave use. The other few Middle Bronze Age cave sites known in eastern Sicily, as Chiusazza (Tinè, 1965), Calafarina (Orsi, 1907b), Gisana (Guzzardi, 1985-1986) and Barriera (Orsi, 1907a), offer a scenario of both ritual and funerary use. In the case of Grotte di Marineo, we could suggest that the use was mainly ritual, since there are no traces of burials or activities related to dwelling.

Experimental

Materials

The main Middle Bronze Age contexts at Grotte di Marineo were represented by the test pit 2 (layers 2-4) and test pit 3 (layer 2) of the Cave 1 and the test pit 1 (layers 4 and 5) of the Cave 3. The study of ceramic materials has brought to the selection of 230 samples that were distinguished through autoptic analysis in three groups: group 1, attested for 22%, is fine, hard and compact, with clay paste color between 2.5 YR 7/3 and 7.5 YR 5/2 brown and few grits smaller than 0.25 mm; group 2, attested for 48%, is semi-fine, hard and compact, with clay paste color between 5 YR 6/6 and 10 Y 6/1 and many grits measuring between 0.25 mm and 1 mm; group 3, attested for 30%, coarse, is soft and porous, with clay paste color between 2.5 YR 7/6 and 5 YR 4/4 and many grits larger than 1 mm.

Basing on the type and frequency of the grits, group 1 and group 2 were both split in four subgroups (1A, 1B, 1C, 1D and 2A, 2B, 2C, 2D) and group 3 in two subgroups (3A e 3B) (Figure 2, Table 2).

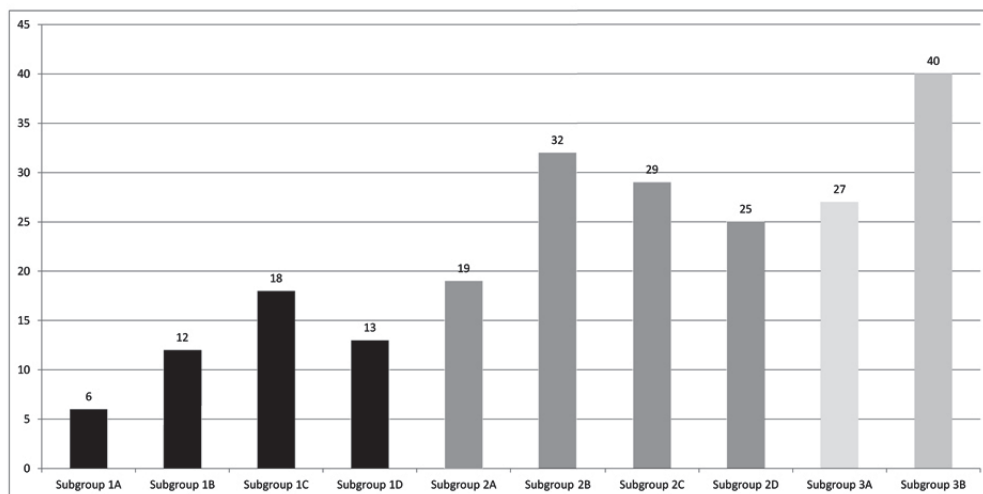


Figure 2. Chart indicating the subgroups presence.

Table 2. Different occurrence of groups and subgroups from autoptic analysis.

Groups	1 (fine)				2 (semi-fine)				3 (coarse)	
	1A	1B	1C	1D	2A	2B	2C	2D	3A	3D
Calcareous	x	x	x	x	x	x	x		x	x
Volcanic	x				x	x	x	x	x	x
Volcanicglass			x							x
Chamotte				x	x					
Pebbles							x			x
Quartz		x				x	x		x	x

With regards to decorative techniques (Figure 3a,b), half of the samples are just burnished, while only a few ceramics are undecorated. Low percentages present the surface with also incision, excision and relief, that are traditionally much more diffused in the Thapsos pottery of Siracusa area. Definitely rare is the slip, that, when present, has been applied both through full immersion and the use of brush. Black blotches due to burning are also present in the 50% of the samples and may be related to the firing method and kiln type.

Finally, repair holes are present on the 18% of the samples which indicate a low technical level in the production or maybe the impossibility of replacing the broken vessels due to the distance from the production center.

With regards to shapes (Figure 4), the most significant element is the high presence of open vessels, mainly cups and basins. Scarcely attested are pouring and dipping vessels, as well as plates and bowls. On the other hand, jars usually coming with discoid lids and cooking pots are numerous. In general, simple and pedestal cups belong to groups 1 and 2, while jars, cooking vessels and some basins are related to group 3.

For each shape, several typologies which can be attributed to the three chronological sub-phases of Thapsos culture, were identified,

although they are not discussed in this contribute. Without precise stratigraphic data, based on the outcome of the typological analysis, it can be inferred that the occupation of the site lasted for all the three sub-phases of Thapsos period, as testified by the chronological interpretation of the main types (Table 3).

To test the interpretative hypotheses about technology based on the autoptic exam and to provide some new data about the archaeometric characterization of Middle Bronze Age pottery, completely missing as above mentioned, 31 samples representing all the subgroups were selected and treated with detailed petrographic description and geochemical analysis (XRF). Furthermore, on 11 samples representative of the three chronological sub-phases of local Bronze Age, small-angle neutron scattering (SANS) and scanning electron microscopy (SEM) analyses have been carried out.

The sample name has been assigned following the archeological clustering: LE stands for Licodia Eubea; the first Arab number (1, 2, 3) recalls the group they belong to; the letter indicates the subgroups and the second number differentiates the specimens.

Methods

Petrographic descriptions on thin sections have been made following the scheme proposed

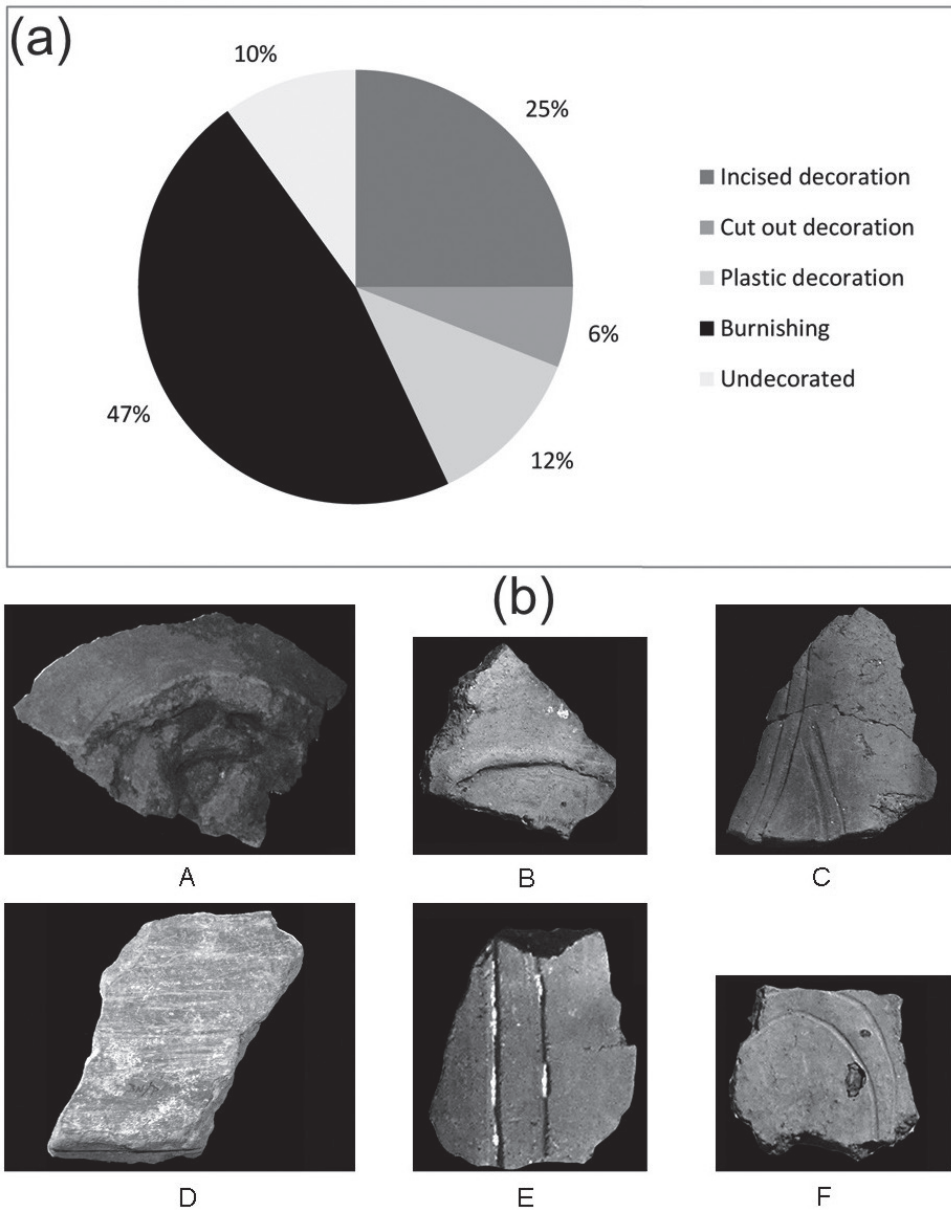


Figure 3. (a) Chart indicating the percentage presence of decorative techniques; (b) Features of Thapsos pottery: A) Finger and palm prints; B) Palette tool signs; C) Tool incision with 'U' and 'V' section points; D) Potter's wheel signs; E) Filling with white paste; F) Superficial voids and cracks.

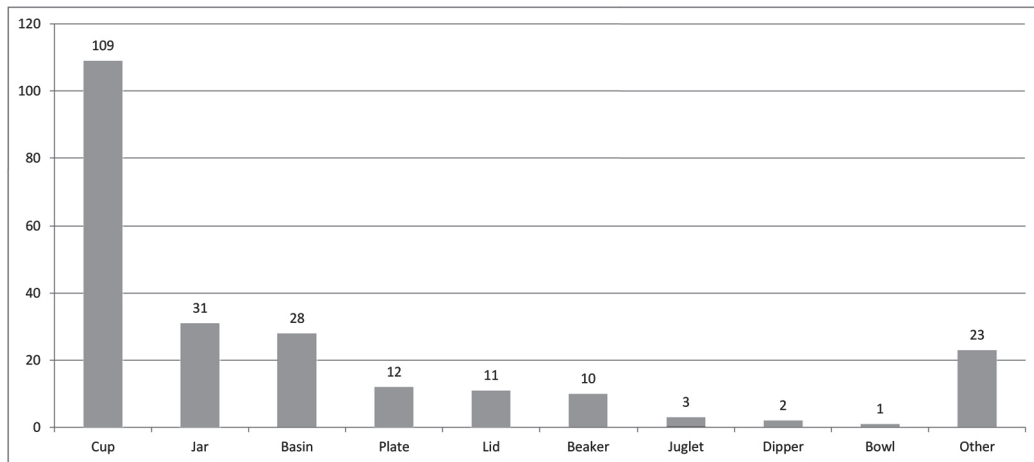


Figure 4. Chart indicating the presence of single shapes within the typological groups.

Table 3. Chronological chart with main pottery types distinguished in the three phases of Thapsos period.

THAPSOS PERIOD	POTTERY TYPES
THAPSOS I (1440/1420-1400-1380 BC)	CUP OF TYPE II (LE1A1, LE1B, LE1B1, LE1C, LE3B) Basin of type I (LE1A2, LE3A, LE3A3)
THAPSOS II (1400/1380-1310-1300 BC)	CUP OF TYPE III (LE1A, LE2A, LE2C1) BASIN OF TYPE II (LE2D, LE2A1, LE3A1)
THAPSOS III (1310/1300-1270-1250 BC)	CUP OF TYPE IV (LE2A2, LE3B1)
	CUP OF TYPE VI (LE1B2, LE1C1, LE1D, LE1D1, LE2A3, LE2B3, LE2B4, LE2C, LE2C3) CUP OF TYPE I (LE2B, LE2B1, LE2B2, LE2C2, LE2D1) JAR OF TYPE IV (LE 3A2)

by Whitbread (Whitbread, 1995), which facilitates a detailed characterization of pottery in terms of texture, groundmass and inclusions.

Chemical analyses of major and trace elements were performed by X-ray fluorescence (XRF) spectrometry (PHILIPS PW 2404/00) on powder-pressed pellets; total loss on ignition (LOI) was gravimetrically estimated after overnight heating at 950. Further information are reported on previous papers (Barone et al., 2013). Micro-morphological investigation of sample have been carried out by using a Tescan Vega LMU scanning electron microscope (SEM). Observation have been performed on small fragments drawn from the samples and attached to an aluminium stub with double-sided tape and coated in carbon.

Finally, SANS measurements were performed on the PAXE spectrometer at the ORPHEE reactor of the Laboratoire Léon Brillouin (LLB, Saclay, France) (<http://www-llb.cea.fr/spectros/spectro/g5-4.html>).

Some basic background about methodology is here reported; further information are in Barbera et al., 2013.

In a SANS experiment, a beam of neutron interact with a samples, determining a low angle scattering intensity $I(Q)$ in function of the exchanged momentum between radiation and particles

$$Q = \frac{4\pi}{\lambda} \sin \frac{\theta}{2}$$

(with: λ = incident neutron wavelength; θ = scattering angle) (Higgins & Benoit 1994),

The intensity of scattering $I(Q)$ is usually expresses as (Teixeira, 1988):

$$I(Q) = \frac{N_p}{V} V_p^2 (\rho_p - \rho_0)^2 P(Q) S(Q) + B_{inc} \quad (1)$$

where N_p is the number concentration of scattering bodies, V_p is the volume of one scattering body, $(\rho_p - \rho_0)$ is the difference in

neutron scattering length density (usually called contrast K), $P(Q)$ is the form or shape factor, $S(Q)$ is the interparticle structure factor, and finally B_{inc} is the (isotropic) incoherent background signal.

The form factor, $P(Q)$ given by Van de Hulst's equation,

$$P(Q) = \frac{1}{V_p^2} \left| \int_0^\infty \exp[i(Q\alpha)] dV_p \right|^2 \quad (2)$$

is a function that describes how $I(Q)$ is modulated by interference effects between radiation scattered by different parts of the same scattering body, where α is a shape parameter that might represent a length or a radius of gyration (R_g).

Interparticle structure factor, given by,

$$S(Q) = 1 + \frac{4\pi N_p}{QV} \int_0^\infty [g(r) - 1] r \sin(Qr) dr \quad (3)$$

is a function that describes how $I(Q)$ is modulated by interference effects due to different scattering bodies. Consequently, it is dependent on the degree of local order in the sample.

In petrography, SANS has been used to demonstrate the fractal character of rocks and determine their fractal dimension (Lucido et al., 1988). Fractals are described as structures with self-similarity proprieties within some spatial range, (i.e., the structure is independent on the length scale of observation in that range) and a fractal dimension.

It is possible prove that the measured scattered intensity $I(Q)$ in a SANS experiment is related to surface fractal dimension of studied particles by the relation:

$$I(Q) = Q^{-(6-D_s)} \quad (4)$$

where D_s is the fractal dimension of studied particles; for fractal surfaces it has to be between 2 and 3. In the study of ceramics, SANS can be used to study the fractal features of newly

formed crystalline aggregates. Real fractal objects scatter according to Eq. (4) only within a limited Q range, i.e., $\xi^{-1} < Q < r_0^{-1}$ where r_0 is the size of single particles in an aggregation process, and ξ the size of the aggregates.

In this experiment, spectra have been collected using two different configurations; large Q : $\lambda = 6\text{Å}$, sample-detector distance = 2 m, collimation = 2 m, and Q -range extending from 5×10^{-3} to $2 \times 10^{-1} \text{Å}^{-1}$; and small Q : $\lambda = 15 \text{Å}$, sample-detector distance = 4.5 m, collimation = 4.5 m, and Q -range extending from 3×10^{-3} to $3 \times 10^{-2} \text{Å}^{-1}$. Samples studied were thin sections (thickness < 1 mm), and therefore problems arising from multiple scattering effects are minimized. No appreciable neutron activation of the samples was found after the experiment. By the standard LLB SANS routines, the two-dimensional intensity distributions were corrected for the background and normalized to absolute intensity by measuring the incident beam intensity, the transmission and the thickness of each sample. By integrating the normalized two-dimensional intensity distribution with respect to the azimuthal angle, we obtained one-dimensional scattering intensity distributions $I(Q)$ expressed as the unit differential cross-section per unit volume of the sample (cm^{-1}).

Results

Petrographic and micro-morphological observations

The optical microscopic analysis allowed to distinguish and characterise six fabrics (Figure 5): fabric A - with abundant limestones inclusions and fossiliferous groundmass (LE1B, LE1B1, LE1B2); fabric B - with volcanic glass inclusions (LE2B2, LE1A and LE2B) and occasionally by limestone (LE2B), the groundmass is scarcely fossiliferous; fabric C - with volcanic glass and quartz inclusion and un-fossiliferous groundmass (LE1C, LE1C1); fabric D - with inclusion formed by

volcanic glass, and limestones, the groundmass is fossiliferous (LE2C3, LE2A); fabric E - characterised by the presence of grog together with volcanic glass and limestone (LE2C1), with volcanic glass and rock fragments (LE1A1, LE1A2, LE1D, LE2B4, LE2D) and with only limestone fragments (LE3B1); in all the samples the groundmass is fossiliferous (LE2C1) or abundantly fossiliferous; fabric F - with volcanic glass, rock fragments and minerals (pyroxenes and plagioclases) and fossiliferous groundmass (LE1D1, LE2A1, LE2A2, LE2A3, LE2B1, LE2B3, LE2C, LE2C2, LE2D1, LE3A, LE3A1, LE3A3, LE3A2).

Most of the described fabrics have as distinguishable feature the presence of volcanic inclusions (more or less weathered glass, rocks and minerals clasts) while the use of grog, widespread in the Ancient Bronze pottery of the neighbouring site of Ramacca (Agodi et al., 2000), is limited to the fabric E. Furthermore, the samples may be distinguished also on the basis of the fossils abundances in the groundmass.

Regarding the optical activity, the samples belonging to the fabrics A, D and E (with the exception of LE3B1) have medium to high birefringence while it is low or absent in the fabrics B, C and F. This data may be used for the firing temperature esteem; in fact, low or absent birefringence is, in many cases, indicative of the achievement of high firing temperature bringing the modifications of the original mineralogical association of the groundmass (mainly clay minerals and calcite) and to the formation of cryptocrystalline new phases (anorthite, diopside, wollastonite and gehlenite).

About the evolution of technological aspects of pottery manufacture through the three chronological sub-phases of Thapsos culture, micro-morphological analysis by scanning electron microscopy (SEM) are carried out in order to provide information on the degree of vitrification reached by the samples studied during firing considering that chemical data

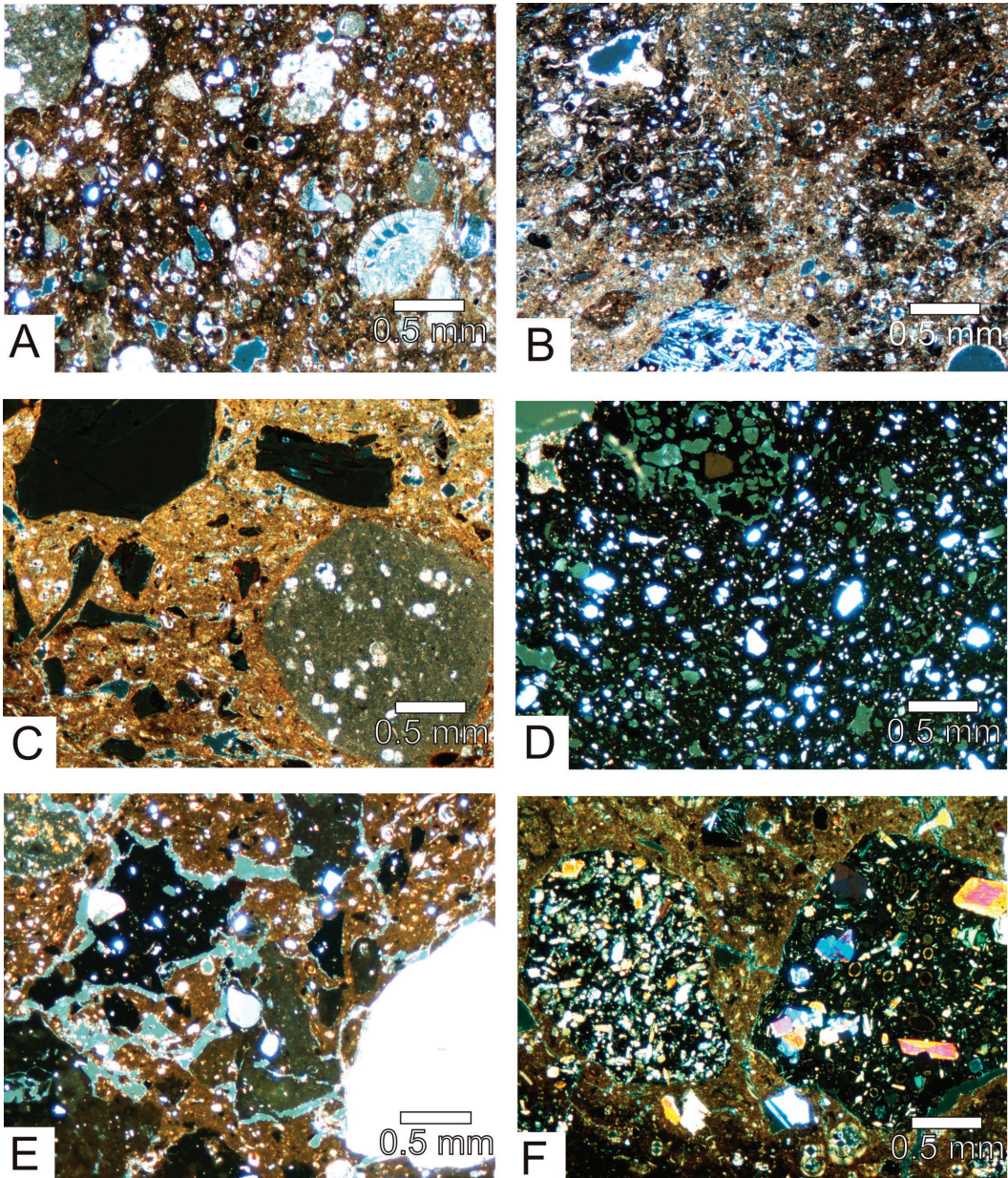


Figure 5. Thin sections of the specimens belonging to the 6 fabrics identified: A) fabric A (LE1B1); B) fabric B (LE1A); C) fabric C (LE2C3); D) fabric D (LE1C1); E) fabric E (LE2C1); F) fabric F (LE2B3).

allowed us to classify all samples as high CaO pottery (CaO > 12 wt%: see Geochemical analysis paragraph). In this regard, samples may be subdivided into three groups whose representative specimens are reported in Figure 6: samples LE 2D (Figure 6a), LE1B, LE 1B2, LE2C, LE3B1 and LE 3A2 show aggregate of flaky clay particles; samples LE 2A (Figure 6b) exhibits an initial vitrification; in LE 2B (Figure 6c) the development of a very high concentration of fine bloating pores is observable in conjunction with the first appearance of initial vitrification; samples LE 1C (Figure 6d), LE 1A, LE 2A1 display extensive vitrification. Finally, the vitrification degree in association with the chemical composition of clay suggest oxidizing firing atmosphere (Maniatis and Tite, 1981). Summarizing, samples belonging to B, C and D fabrics exhibit from intermediate to extensive vitrification degree, while samples of fabrics A, E and F show a flaky clay structure.

Small Angle Neutron Scattering

Mesoscopic and structural characteristics of the analyzed samples were studied by SANS measurements. The interpretation of SANS spectra is performed in terms of two independent populations of mesoscopic structures (big units imputable to newly formed minerals crystallites and small units attributed to voids/mineral aggregates) with substantially different radii. Their contributions to the scattering law are additive, and hence can be fitted according to (Beaucage, 1995):

$$I Q \cong C_1 \exp\left(-\frac{Q^2 R_g^2}{3}\right) + C_2 Q^{-\alpha} \quad (5)$$

The prefactors $C1$ and $C2$ are free parameters containing the relative intensity of Guinier's and power law. The two free parameters, the radius of gyration R_g and the exponent $\alpha = 6-D_s$, are indicative of the mean size of newly formed minerals crystallites and the roughness of the aggregates, respectively. As previously

discussed, surfaces that exhibit a fractal behavior have D_s value between 2 and 3, then the parameter α must be between 3 and 4. The two-dimensional Euclidean exponent $D_s = 2$ ($\alpha = 4$) is recovered for particles with sharp interfaces while $D_s = 3$ ($\alpha = 3$) testify particles with smooth interface. Figure 7 displays, for example, the SANS spectra of sample LE1C together with the best-fit according to the above equation. The obtained values of R_g and α for all the investigated archaeological samples are reported in Table 4.

As far as the fractal exponent α is concerned, its value ranges between 3 and 4, in agreement with the fractal surface model, revealing an interface of structural rearrangement reactions with fingered fractal geometry (Barbera et al., 2013). In detail, as can be seen in Figure 8, the α values range from 3.13 to 3.66 with relation to the petrographic classification; the highest values are revealed for B, C and D fabrics, whereas fabrics A, E and F have, on average, lower values. This evidence is coupled with vitrification degree SEM results.

Starting from the obtained surface fractal dimension (α), a first estimation of the maximum firing temperature (T_{max}) has been achieved by using by using a master plot, previously constructed (Barone et al., 2009) for a set of reference samples fired under controlled conditions (Plio-Pleistocenic Clays) which our findings appear to be similar to as far as chemical composition is concerned (see geochemical analysis paragraph) and already successfully applied to pottery specimens. Hence, we connected the α exponent of samples to T_{max} as shown in Figure 9.

The extracted T values are plotted in Figure 10, together with the firing max temperature obtained by means of SEM and XRD, the latter ones reported in literature for the same samples (Barone et al., 2011a).

Worthy of note is that the T_{max} values estimated by the SANS technique are in good

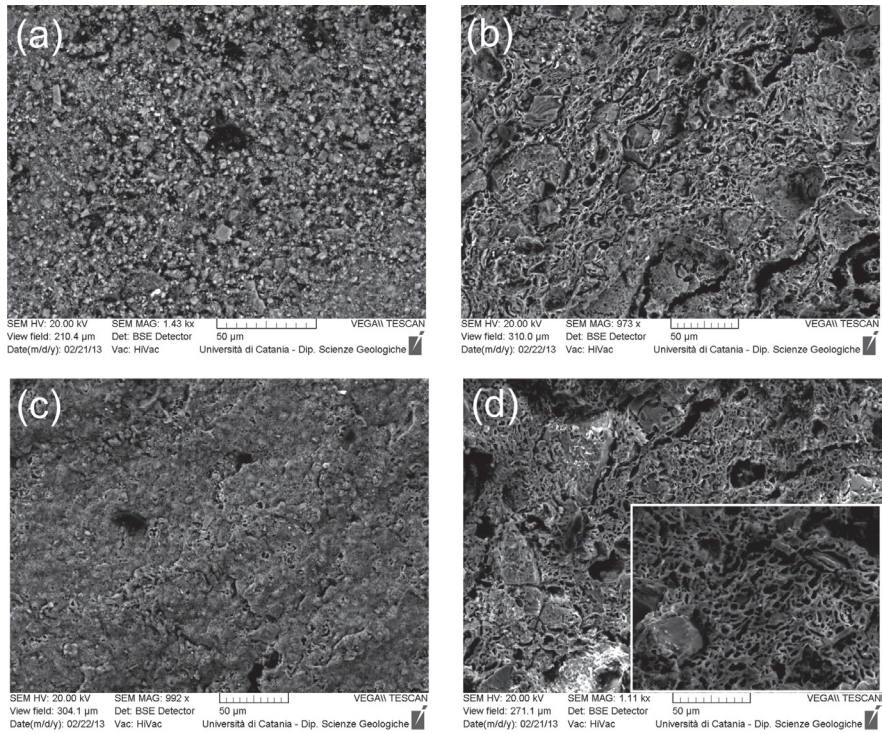


Figure 6. SEM photographs of: (a) Unvitrified structure (LE2D), (b) Partially vitrified structure (LE2A), (c) bloating structure (LE2B) and vitrified structure (LE1C).

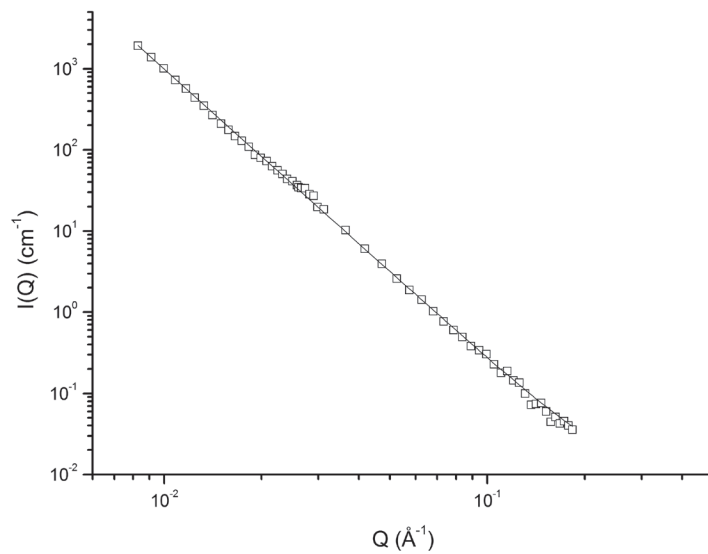


Figure 7. Scattered SANS intensity (open squares) for sample LE1C together with the best-fit (continuous line).

agreement with those obtained by the other considered methods (Table 5), suggesting that small angle neutron scattering may be used as a non-invasive method for the study of pottery production technology.

Geochemical analysis

The chemical composition of the samples belonging to the six petrographic fabric (A-F) are reported on Table 6. The data were treated with the statistical methodology mainly based on the log-ratio technique introduced by Aitchison (Aitchison, 1986) and employed in order to avoid the constant sum problem; the centred log-ratio transformation (clr) of data is applied as follows: $x \in SD \rightarrow y = \ln(xD / gD(x)) \in RD$ where x is the vector of the D elemental compositions, y is the vector of the log-transformed compositions, $xD = (x_1, x_2, \dots, x_D)$ and $gD(x) = (x_1 \cdot x_2 \cdot \dots \cdot x_D)^{1/D}$. This operation transforms the raw data from their constrained sample space, the simplex $S_d(d = D - 1)$, into the real space R_d , in which parametric statistical methods can be applied to the transformed data. Subsequently, the clr-transformed data set was explored by biplots, a graphical representation of variables

and cases projected on to principal components planes. Both the clr-transformation and the biplot calculations were obtained by using CoDaPack (Thiò-Henestrosa, 2005), a compositional software that implements the basic methods of analysis of compositional data based on log-ratios, following the methodology introduced by Aitchison (Aitchison, 1986) widely used in the archaeometric study (Aitchison et al., 2002; Buxeda i Garrigós, 1999; Barone et al., 2005; Barone et al., 2011c; Barone et al., 2011d; Barone et al., 2012). The biplot of Figure 11 represents the elements and the studied samples plotted in the first two principal component plane. It explain the 69% of the total variance of major and trace elements used for the log-ratio transformation (major elements: CaO, MgO, MnO, Fe₂O₃, K₂O; minor elements: Zr, Rb, Ba, Sr, Ni, Co, Cr). On the whole, there is a good correspondence among the petrographic observations and the samples clusters obtained in the biplot: a) the CaO abundance is discriminant between the very fossiliferous fabric A and the scarcely fossiliferous fabrics B and C; b) the abundance of volcanic inclusions separates the fabric F samples from the fabric E on the basis of

Table 4. Radius of gyration R_g and fractal dimension α for all the investigated samples. (Lo) and (Tr) refer to longitudinal and transversal configurations.

Sample	R_g (Å)	α
LE1A	123.1	3.66
LE 1B	122.8	3.24
LE 1B2	99.8 (Lo) - 103.7 (Tr)	3.29 (Lo) - 3.25 (Tr)
LE 1C	127.7 (Lo) - 249.9 (Tr)	3.56 (Lo) - 3.56 (Tr)
LE 2A	90.4	3.43
LE 2A1	114.3 (Lo) - 118.5 (Tr)	3.52 (Lo) - 3.52 (Tr)
LE 2B	133.0 (Lo) - 144.1 (Tr)	3.65 (Lo) - 3.60 (Tr)
LE 2C	80.7 (Lo) - 80.7 (Tr)	3.41 (Lo) - 3.41 (Tr)
LE 2D	118.5	3.20
LE 3A2	93.4	3.18
LE 3B1	100.4 (Lo) - 97.2 (Tr)	3.13 (Lo) - 3.23 (Tr)

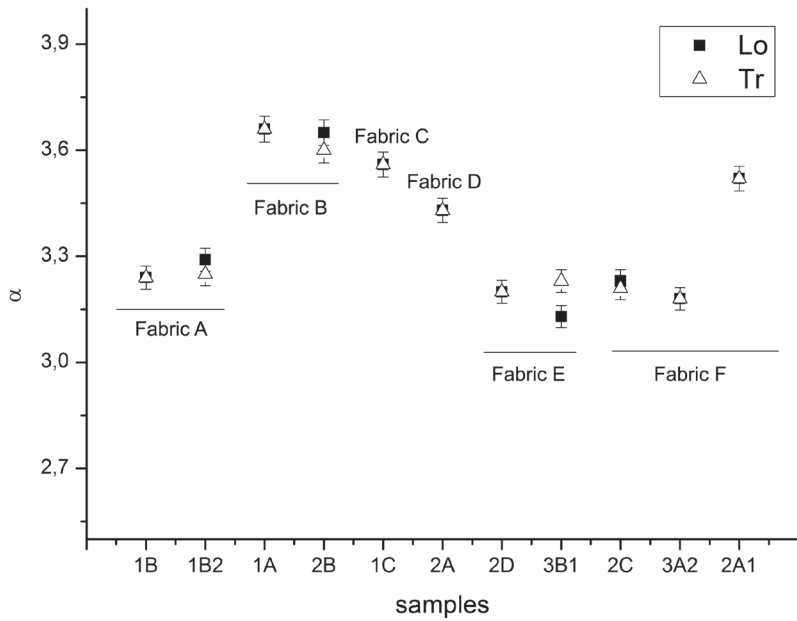


Figure 8. α values for all the investigated samples.

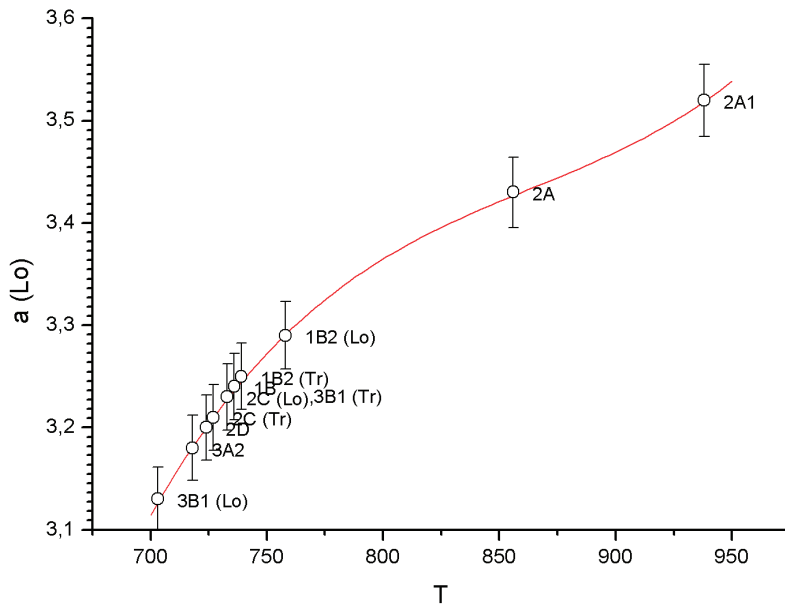


Figure 9. Temperature dependence of the fractal exponent α for LE samples plotted on AP# reference clays (Barone et al., 2009). Error bars on values are of the order of 1%. Lo refer to longitudinal configuration; Tr refer to transversal configuration.

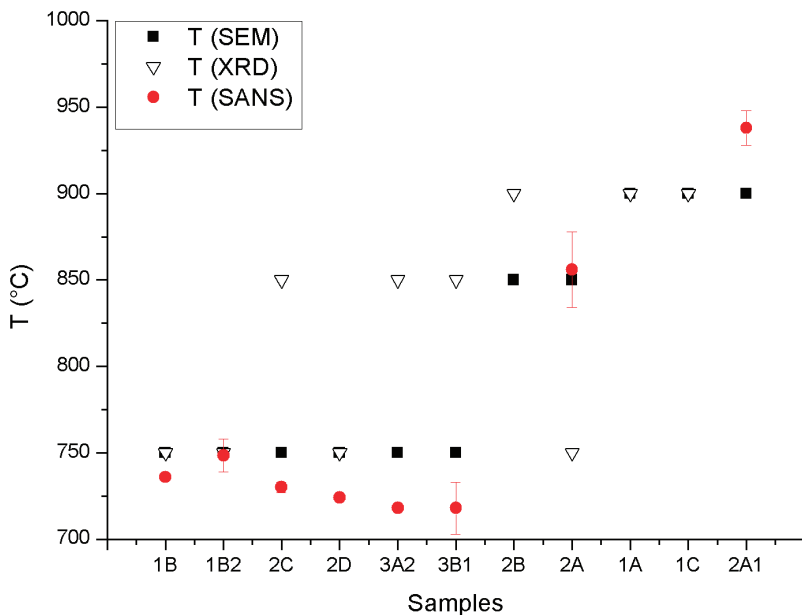


Figure 10. Comparison among the firing temperatures estimated by SANS (circles), XRD (triangles) and SEM (squares) techniques.

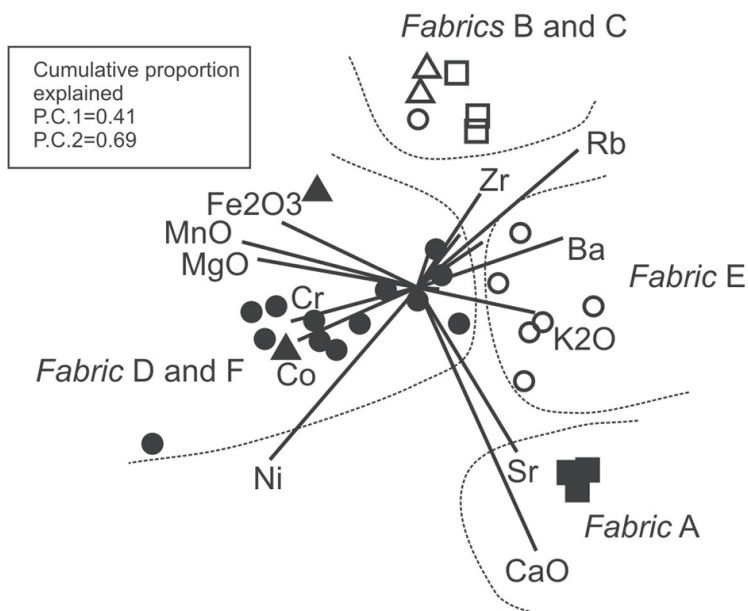


Figure 11. Biplot of the two principal components.

Table 5. Maximum firing temperature T_{max} of the analysed archaeological pottery esteemed on the basis of mineralogical association (XRD), vitrification degree (SEM) and α values as obtained from the α vs. T master plot reported in (Barone et al., 2009) (see text for details).

Fabric	Sample	BIREFRINGENCE	Qtz	CM	Cc	Pl	Cpx	Zeo	Geh	An	Di	Hm	T°C (XRD)	T°C (SEM)	T°C (SANS)
FABRIC A	1B	low	+++	+++	+++	+							< 800	< 800	736
	1B2	low	+++	+++	+++	+							< 800	< 800	749
FABRIC B	1A	medium-high	+++	+	+	+	+	+	+	++	++		900	> 900	-
	2B	medium-high	+++	+	+	+	+	+	+	++	++	+	900	800-900	-
FABRIC C	1C	medium-high	+++	+	+	+	+	+	++	++	++		900	> 900	-
FABRIC D	2A	low	+++	++	+++	+	+						< 800	800-900	856
FABRIC E	2D	low	+++	+++	+++			+					< 800	< 800	724
	3B1	medium-high	+++	+	++	+	+	+	+	++	++	+	800-900	< 800	718
FABRIC F	2C	medium-high	+++	+	++	+				++	++		800-900	< 800	730
	2A1	medium-high	+++	+	++	+			+	++	++		-	-	938
	3A2	medium-high	+++	+	++	+			+++	+++	+++	++	800-900	< 800	718

Qtz = quartz; CM = clay minerals; Cc = calcite; Pl = plagioclase; Cpx = clinopiroxene; Zeo = zeolite; Geh = gehlenite; An = anorthite; Di = diopside; Hm = hematite; +++ = abundant; ++ = present; + = scarce.

Table 6. Chemical composition of the samples belonging to the six petrographic fabric (A-F). Major element are reported in wt%, minor elements in ppm.

Fabric	Sample	SiO ₂	TiO ₂	Al ₂ O ₃	Fe ₂ O ₃	MnO	MgO	CaO	Na ₂ O	K ₂ O	P ₂ O ₅
A	LE1B	39.09	0.33	11.18	2.05	0.03	0.94	30.39	0.37	2.98	0.28
A	LE1B1	39.02	0.33	11.19	2.05	0.03	0.89	30.70	0.36	2.94	0.26
A	LE1B2	38.64	0.34	11.51	2.16	0.03	0.98	32.50	0.37	3.19	0.26
B	LE2B2	54.70	0.74	32.79	6.38	0.08	2.56	13.29	1.04	3.91	0.53
B	LE1A	57.25	0.80	35.86	6.46	0.11	2.56	11.91	0.81	3.08	0.52
B	LE2B	55.04	0.76	34.88	6.59	0.08	2.84	12.85	0.77	3.82	0.47
C	LE1C	59.09	0.79	35.53	6.24	0.11	2.65	12.16	0.65	2.79	0.40
C	LE1C1	59.93	0.78	35.27	6.09	0.11	2.51	12.00	0.65	2.68	0.39
D	LE2A	55.50	1.02	27.73	7.43	0.12	3.23	14.75	0.77	2.00	0.69
D	LE2C3	49.99	0.85	20.05	5.80	0.08	2.34	18.55	0.84	2.93	0.30
E	LE2C1	50.71	0.60	25.98	4.34	0.06	1.62	20.63	0.49	3.56	0.23
E	LE3B	48.31	0.48	20.75	3.44	0.04	1.64	21.48	0.27	3.33	0.34
E	LE1A1	48.24	0.49	21.52	3.73	0.04	1.46	21.39	0.30	4.14	0.42
E	LE1A2	48.85	0.60	21.23	4.13	0.05	1.89	20.46	0.46	3.43	0.34
E	LE3B1	55.05	0.77	31.15	6.21	0.11	2.44	12.70	0.90	3.99	0.66
F	LE1D	51.02	0.66	25.81	4.79	0.05	1.92	18.88	0.45	3.83	0.34
F	LE1D1	52.01	0.82	28.18	6.19	0.07	2.43	17.51	0.58	3.33	0.52
F	LE2A1	50.34	0.76	26.78	5.97	0.07	2.38	19.67	0.58	3.41	0.60
F	LE2A2	50.91	0.86	21.69	5.84	0.09	2.71	19.84	0.69	2.47	0.19
F	LE2A3	50.13	0.83	22.33	5.77	0.09	1.95	20.61	0.46	3.04	0.25
F	LE2B1	51.01	0.76	23.85	5.38	0.06	1.94	17.55	0.48	3.39	0.43
F	LE2B3	48.39	1.07	21.68	7.36	0.10	4.24	18.29	0.65	2.33	0.66
F	LE2B4	45.13	0.45	15.62	3.01	0.04	1.59	25.41	0.46	3.60	0.40
F	LE2C	49.33	0.95	23.84	7.48	0.11	3.48	18.77	0.81	2.77	0.53
F	LE2C2	47.67	0.83	22.54	6.50	0.09	2.85	22.87	0.57	2.31	0.35
F	LE2D	47.55	0.46	19.43	3.28	0.04	0.93	21.96	0.35	4.11	0.48
F	LE2D1	51.45	0.96	23.12	6.59	0.09	2.26	16.02	0.47	3.27	0.39
F	LE3A	46.28	0.79	20.84	6.49	0.09	2.82	22.98	0.61	3.21	0.76
F	LE3A1	49.90	0.97	25.74	7.66	0.10	3.70	18.70	0.75	2.56	0.60
F	LE3A3	50.60	0.82	23.40	6.07	0.09	2.59	17.64	0.55	3.74	0.52
F	LE3A2	44.05	0.90	15.40	6.51	0.11	3.72	23.69	0.91	2.83	0.60

Table 6. Continued...

Fabric	Sample	Sr	V	Cr	Co	Ni	Zn	Rb	Y	Zr	Nb	Ba	La	Ce
A	LE1B	678	40	52	17	52	47	33	15	92	11	179	31	43
A	LE1B1	688	38	53	15	53	45	31	15	90	12	205	31	66
A	LE1B2	722	38	54	16	56	45	33	16	91	11	205	27	53
B	LE2B2	659	87	100	31	44	78	95	27	160	19	456	31	79
B	LE1A	476	93	103	25	42	83	89	29	207	19	292	42	90
B	LE2B	693	84	106	30	47	85	100	28	173	20	348	37	90
C	LE1C	410	81	103	27	47	70	82	30	234	19	271	32	77
C	LE1C1	402	81	96	26	48	71	80	30	226	17	260	32	75
D	LE2A	521	87	138	38	93	65	51	28	197	35	332	42	106
D	LE2C3	558	56	114	36	81	65	34	18	96	12	130	25	61
E	LE2C1	510	84	86	26	47	55	68	26	143	17	290	32	78
E	LE3B	666	60	75	24	50	64	65	26	99	12	144	29	75
E	LE1A1	710	62	85	24	46	57	62	21	118	15	206	29	54
E	LE1A2	702	59	98	27	62	64	51	19	112	16	247	26	59
E	LE3B1	415	83	100	28	55	74	81	29	172	20	288	36	76
F	LE1D	739	73	102	30	61	66	65	24	136	18	286	34	70
F	LE1D1	750	82	125	30	70	74	70	27	149	19	261	33	83
F	LE2A1	759	81	121	29	71	70	69	25	145	20	238	36	78
F	LE2A2	522	63	123	36	89	59	36	19	119	15	156	23	32
F	LE2A3	569	54	105	34	77	61	47	20	132	15	175	27	57
F	LE2B1	644	63	121	31	68	72	50	22	120	16	258	28	59
F	LE2B3	799	87	200	45	151	67	37	25	149	40	259	55	116
F	LE2B4	801	68	80	19	44	51	42	18	95	13	210	28	51
F	LE2C	619	72	154	43	102	76	45	22	115	18	169	29	57
F	LE2C2	581	64	139	38	108	69	49	21	115	17	241	34	66
F	LE2D	681	59	74	21	35	56	56	19	109	14	304	29	47
F	LE2D1	578	56	143	39	87	72	39	19	107	18	197	31	68
F	LE3A	719	73	129	39	95	68	51	21	115	17	210	26	66
F	LE3A1	758	76	157	46	98	74	53	21	125	18	204	31	57
F	LE3A3	657	77	134	38	83	65	42	21	117	17	582	25	76
F	LE3A2	586	71	156	46	128	61	22	17	85	14	114	18	47

Fe₂O₃, MgO, MnO, Cr, Co e Ni contents. On the basis of these results, it is possible to suppose the use of different raw materials as is evident from the samples of fabric A and the samples of fabrics B and C.

Discussion

The petrographic analysis permitted to surpass the previous autoptic exam of the Grotte di Marineo ceramic production that allowed the recognition of three groups (1-3) and evidenced the presence of 6 fabrics (A-F) on the basis of inclusions and groundmass. Referring to the potential raw materials used in the production process, the inclusions and the groundmass are compatible with geological materials cropping out in the Licodia Eubea area (Grasso et al., 2004). In particular, the volcanic rock fragments exhibit a mineralogical composition and structural features similar to the Plio-Pleistocene alkali basalts and tholeiites (Beccaluva et al., 1998; Di Grande et al., 2002) while the weathered volcanic glass resembles the Pliocene palagonitised submarine volcanites outcropping in Licodia Eubea neighbouring.

Finally, the mudrocks of the Miocenic Tellaro Formation and/or the Quaternary alluvium may be supposed as the clay raw material. Some relevant considerations on the relationship between fabric and chronology: i) fabrics A and C seem to be exclusive of shapes of Thapsos I phase (1440/1420-1400/1380 BC); ii) fabrics D just attested and E mainly are attested on samples of Thapsos II phase (1400/1380-1310/1300 BC); iii) fabrics B and F occurring just on those of Thapsos III phase (1310/1300-1270/1250 BC). This correlations suggest technical, other than stylistic, changes attested by the different fabrics used in the course of the chronological development of Middle Bronze Age (Table 7). The hypothesis that these modification in the pottery production is the effect of some technical achievement, due to an experimentalism that

took place during the Thapsos period, seems just apparently contradicted by the esteem of firing temperature.

In fact, the firing temperature esteemed by petrographic analysis, SEM observation and SANS measurements are in agreement with the results obtained by previous X-ray diffraction (XRD) measurements and infra-red spectroscopy (FT-IR) (Barone et al., 2011a). It is worth noting that, the presence of diopside in the mineralogical analysis of samples exhibiting volcanic tempers cannot be directly used as temperature fingerprint. In these case. information about

Table 7. Comparative chart between specimens, fabrics and relative chronology.

Chronology	Sample	Fabric
Thapsos I	LE1B	
Thapsos I	LE 1B1	A
Thapsos I	LE 1B2	
Thapsos II-III	LE 2B2	
Thapsos II	LE 1A	B
Thapsos II-III	LE 2B	
Thapsos I	LE 1C	
Thapsos I	LE 1C1	C
Thapsos II	LE 2A	
Thapsos I	LE 2C3	D
Thapsos II	LE 2C1	
Thapsos I	LE 3B	
Thapsos I	LE 1A1	E
Thapsos II	LE 2D	
Thapsos I	LE 2B4	
Thapsos I	LE 1D	
Thapsos III	LE 3B1	
Thapsos III	LE 2A2	
Thapsos II	LE 2C	
Thapsos II	LE 3A1	F
Thapsos II-III	LE 3A2	

firing temperature have been extracted by SEM and SANS results. Moreover, the unique values of temperature give back by SANS analysis is due to one-to-one correlation; an interval around the given value should be considered.

In detail, the fabrics A, D and E underwent to relatively low firing temperature (< 800 °C), samples belonging fabrics B and C are characterized by higher firing temperatures (~ 900 °C) while, the samples of fabric F underwent to intermediate conditions (800-900 °C), even if they show no-vitrification stage in spite of presence of calcium aluminum silicates (i.e. gehlenite) (see Table 5).

These considerations introduce the main archaeological research question: how can it be explained the use of 6 different fabrics, sometimes coexisting and with fluctuating firing temperatures, at Grotte di Marineo along the course of the Thapsos period?

Assuming that all the materials found at Grotte di Marineo has come from the same production center one first option can be that the potters preferred some fabrics to others, changing from phase to phase in order to improve the production, despite to firing temperature depending just on the type of kiln used. In this case the differences in the fabrics can be due to experiments of changing clay sources or modifying the added tempers.

Furthermore, the new scenario about different firing temperatures, high and low, all in use during the three Thapsos sub-phases contradicted the common idea of an escalation of firing temperature from the beginning to the end of Thapsos period, opening new perspective for further studies on Sicilian prehistoric ceramics.

Conclusions

The aim of the present research is to obtain fabrics characterization and technological information of Thapsos production applying,

in conjunction with traditional approach, innovative methodologies such as SANS.

In this context, this study shows as small angle neutron scattering can be used as diagnostic method in determining firing temperature, highlighting the potential of this technique in the technological characterization of ancient pottery. In fact, all the obtained results are in good agreement with the degree of vitrification observed by means SEM analysis and are also comparable with those from traditional techniques, such as XRD, FT-IR and petrographic analyses.

From an archeological point of view, this research has been to have disclosed a wide scenario of cultural perspective and further interpretations on the evidence of Grotte di Marineo that could have been hidden without the contribution of the archaeometric analyses. With regards to Middle Bronze Age pottery of Catania territory, what has been achieved is not enough to characterize an Aetnean production but the research project is not yet over.

Acknowledgements

The authors would like to thank two anonymous reviewer for providing insightful comments and precious improvements to the present paper.

References

- Agodi S., Gueli A.M., Mazzoleni P., Mege D., Procelli E., Sapuppo L. and Troja S.O. (2000) - Il villaggio dell'Antico Bronzo di c. da Torricella: un progetto per lo studio e la datazione dei materiali, *Bollettino dell'Accademia Gioenia di Scienze Naturali in Catania*, 33.257, 175-186.
- Aitchison J. (1986) - The statistics analysis of compositional data, Chapman and Hall, London.
- Aitchison J., Barceló-Vidal C. and Pawlowsky-Glahn V. (2002) - Some comments on compositional data analysis in archaeometry, in particular the fallacies in

- Tangri and Wright's dismissal of log-ratio analysis. *Archaeometry*, 44, 295-304.
- Barbera G., Barone G., Crupi V., Longo F., Maisano G., Majolino D., Mazzoleni P., Teixeira J. and Venuti V. (2013) - Small angle neutron scattering study of ancient pottery from Syracuse (Sicily, Southern Italy). *Journal of Archaeological Science*, 40, 983-991.
- Barone G., Lo Giudice A., Mazzoleni P. and Pezzino A. (2005) - Chemical characterization and statistical multivariate analysis of ancient pottery from Messina, Catania, Lentini and Siracusa (Sicily). *Archaeometry*, 47, 745-762.
- Barone G., Crupi V., Majolino D., Mazzoleni P., Teixeira J. and Venuti V. (2009) - Small angle neutron scattering as fingerprinting of ancient potteries from Sicily (Southern Italy). *Journal of Applied Physics*, 106, 054904.
- Barone G., Crupi V., Longo F., Majolino D., Mazzoleni P., Tanasi D. and Venuti V. (2011a) - FT-IR spectroscopic analysis to study the firing processes of prehistoric ceramics. *Journal of Molecular Structure*, 993, 147-150.
- Barone G., Mazzoleni P., Tanasi D. and Veca C. (2011b) - La tecnologia della produzione ceramica nel Bronzo Medio siciliano: il caso dei pithoi di Monte San Paolillo (Catania). *Rivista di Scienze Preistoriche*, 61, 175-198.
- Barone G., Mazzoleni P., Ingoglia C. and Vanaria M.G. (2011c) - Archaeometric evidences of the 4th-2nd century B.C. amphorae productions in north eastern Sicily. *Journal of Archaeological Science*, 38, 3060-3071.
- Barone G., Crupi V., Longo F., Majolino D., Mazzoleni P., Venuti V., and Aquilia E. (2011d) - Potentiality of non destructive XRF analysis for the determination of Corinthian B amphorae provenance. *X-Ray Spectrometry*, 40, 333-337.
- Barone G., Mazzoleni P., Spagnolo G. and Aquilia E. (2012) - The Transport Amphorae of Gela: A Multidisciplinary Study on Provenance and Technological Aspects. *Journal of Archaeological Sciences*, 39, 11-22.
- Barone G., Mazzoleni P., Aquilia A. and Barbera G. (2013) - The Hellenistic and Roman Syracuse (Sicily) fine pottery production explored by chemical and petrographic analysis. *Archaeometry*, 10.1111/j.1475-4754.2012.00727.x.
- Beaucage G. (1995) - Approximations leading to a unified exponential/power-law approach to small-angle scattering. *Journal of Applied Crystallography* 28, 717-728.
- Beccaluva L., Siena F., Coltorti M., Di Grande A., Lo Giudice A., Macciotta G., Tassinari R. and Vaccaro C. (1998) - Nephelinitic to tholeiitic magma generation in a transtensional tectonic setting: an integrated model for the Iblean volcanism, Sicily. *Journal of Petrology*, 39, 1547-1576.
- Branciforti M.G. (1999) - Siti e insediamenti nella regione etnea in Magna Grecia e Sicilia, stato degli studi e prospettive di ricerca (eds): Barra Bagnasco M., De Miro E., Pinzone A., Bretschneider, Roma, 241-258.
- Buxeda i Garrigós J. (1999) - Alteration and contamination of archaeological ceramics: the perturbation problem. *Journal of Archaeological Science*, 26, 295 - 313.
- Consoli A. (1988-1989) - Licodia Eubea: ritrovamenti preistorici in Contrada Marineo, Beni Culturali Ambientali Sicilia, BCA Sicilia, 9-10, 84.
- Di Grande A., Mazzoleni P., Lo Giudice A., Beccaluva L., Macciotta G. and Siena F. (2002) - Subaerial Plio-Pleistocene volcanism in the geo-petrographic and structural context of the north-central Iblean region (Sicily). *Periodico di Mineralogia*, 71, 159-189.
- Grasso M., Behncker B., Di Geronimo I., Giuffrida S., La Manna F., Maniscalco R., Pedley H.M., Raffi S., Schmincke H.U., Strano D. and Sturiale G. (2004) - Carta geologica del settore Nord-Occidentale dell'Avampae Ibleo e del Fronte della Falda di Gela, Catania.
- Guzzardi L. (1985-1986) - Nuovi dati sulla cultura di Thapsos nel Ragusano, *Archivio Storico per la Sicilia Orientale*, 81-82, 219-240.
- Higgins J.S. and Benoit H.C. (1994) - Polymers and Neutron Scattering. Place Clarendon Press, Oxford.
- La Rosa V. (2004) - Le presenze micenee nel territorio siracusano: per una storia del problema, in Le presenze micenee nel territorio siracusano (eds.): V. La Rosa, A. Ausilio, Padova, 11-20.
- Leighton R. (1986) - Paolo Orsi (1859-1935) and the prehistory of Sicily. *Antiquity*, 60, 15-20.
- Levi S.T. and Jones R.E. (2005) - Analisi archeometriche delle ceramiche in Villaggio dell'età del Bronzo Medio di Portella a Salina nelle Isole

- Eolie, Istituto italiano di preistoria e protostoria (eds): M.C. Martinelli, Firenze, 241-262.
- Lucido G., Triolo R. and Caponetti E. (1988) -Fractal approach in petrology: Small-angle neutron scattering experiments with volcanic rocks. *Physical Review B* 38(13): 9031-9034.
- Maniatis Y. and Tite M.S. (1981) - Technological Examination of Neolithic-Bronze Age Pottery from Central and Southeast Europe and from the Near East. *Journal of Archaeological Science*, 8, 59-76.
- Orsi P. (1907a) - Necropoli e stazioni sicule di transizione. VII. Caverne di abitazione a Barriera di Catania. *Bullettino di Paleontologia Italiana*, 33, 53-99.
- Orsi P. (1907b) - La grotta di Calafarina presso Pachino (Siracusa), abitazione e sepolcro. *Bullettino di Paleontologia Italiana*, 33, 7-22.
- Privitera F. (2010) - I disiecta membra delle età più antiche in Tra lava e mare. Contributi all'archaiologia di Catania (eds): V. La Rosa, M. G. Branciforti, Catania, Novamusa, 45-62.
- Procelli E.(1992) - Appunti per una topografia di Catania pregreca. *Kokalos*, 38, 69-78.
- Procelli E.(2007) - Il territorio di Catania: le grotte di Barriera in Ima Tartara. Preistoria e leggenda delle grotte etnee (eds): F. Privitera, V. La Rosa, Regione Sicilia, Palermo, 225-229.
- Tanasi D. (2008) - La necropoli protostorica di Montagna di Caltagirone (CT), Polimetrica, Monza, 198.
- Tanasi D. (2010) - Gli scavi di Monte S. Paolillo e le presenze di tipo egeo nel territorio di Catania in Tra lava e mare. Contributi all'archaiologia di Catania (eds): La Rosa V., Branciforti M.G., Novamusa, Catania, 81-94.
- Teixeira J. (1988) - Small-angle scattering by fractal systems. *Journal of Applied Crystallography*, 21, 781-785.
- Thió-Henestrosa S. and Martín-Fernández J.A. (2005) - Dealing with compositional data: the freeware CoDaPack. *Mathematical Geology*, 37, 773-793.
- Tinè S. (1965) - Gli scavi nella Grotta della Chiusazza. *Bullettino di Paleontologia Italiana*, 69, 113-286.
- Whitbread I. K. (1995) - Greek Transport Amphorae. A Petrological and Archaeological Study, The British School at Athens, Athens.
- Williams J.L., Levi S.T. (2000) - Archeometria della ceramica eoliana: nuovi risultati, sintesi e prospettive in Studi di preistoria e protostoria in onore di Luigi Bernabò Brea (eds): M.C. Martinelli, U. Spigo, Regione Sicilia, Messina, 265-304.

Submitted, April 2014 - Accepted, October 2014